Microlens OGLE-2005-BLG-169 Implies Cool Neptune-Like Planets are Common

A. Gould[1,6], A. Udalski[2,7], D. An[1,6], D.P. Bennett[4,5,8], A.-Y. Zhou[9], S. Dong[1,6], N.J. Rattenbury[4,10], B.S. Gaudi[1,11], P.C.M. Yock[4,12], I.A. Bond[4,13], G.W. Christie[1,14], K. Horne[3,5,15], J. Anderson[16], K.Z. Stanek[1,6]

and

D.L. DePoy[6], C. Han[17], J. McCormick[18], B.-G. Park[19], R.W. Pogge[6], S.D. Poindexter[6]

(The μFUN Collaboration),

I. Soszyński[7,20], M.K. Szymański[7], M. Kubiak[7], G. Pietrzyński[7,20], O. Szewczyk[7], Ł. Wyrzykowski[7,21], K. Ulaczyk[7], B. Paczyński[22]

(The OGLE Collaboration)

D.M. Bramich[5,21], C. Snodgrass[23], I.A. Steele[24], M.J. Burgdorf[24], M.F. Bode[24]

(The RoboNet Collaboration)

C.S. Botzler[4,12], S. Mao[10], S.C. Swaving[4,12]

[1]Microlensing Follow Up Network (μFUN)

[2]Optical Gravitational Lens Experiment (OGLE)

[3]RoboNet Collaboration

[4]Microlensing Observations for Astrophysics (MOA) Collaboration

[5]Probing Lensing Anomalies NETwork (PLANET) Collaboration

[6]Department of Astronomy, Ohio State University, 140 W. 18th Ave., Columbus, OH 43210, USA; deokkeun,depoy,dong,gould,pogge,kstanek,sdp@astronomy.ohio-state.edu

[7]Warsaw University Observatory, Al. Ujazdowskie 4, 00-478 Warszawa, Poland; udalski,soszynsk,msz,mk,pietrzyn,szewczyk,wyrzykow,kulaczyk@astrouw.edu.pl

[8]Department of Physics, Notre Dame University, Notre Dame, IN 46556, USA; bennett@nd.edu

[9]Department of Physics, Astronomy and Materials Science, Missouri State University, 901 S. National, Springfield, MO 65897 USA; ayz989f@missouristate.edu

[10]Jodrell Bank Observatory, The University of Manchester, Macclesfield, Cheshire SK11 9DL, United Kingdom; njr,smao@jb.man.ac.uk

[11]Harvard-Smithsonian Center for Astrophysics, 60 Garden Street, Cambridge, MA 02138; sgaudi@cfa.harvard.edu

[12]Department of Physics, University of Auckland, Private Bag 92019, Auckland, New Zealand; c.botzler,s.swaving,p.yock@auckland.ac.nz

[13]Institute of Information and Mathematical Sciences, Massey University, Private Bag 102-904, North Shore Mail Centre, Auckland, New Zealand; i.a.bond@massey.ac.nz

[14]Auckland Observatory, Auckland, New Zealand, gwchristie@christie.org.nz

[15]SUPA, Physics & Astronomy, North Haugh, St Andrews, KY16 9SS, UK; kdh1@st-andrews.ac.uk

[16]Dept. of Physics and Astronomy, MS-108, Rice University, 6100 Main Street, Houston, TX-77005, USA; jay@eeyore.rice.edu

[17]Department of Physics, Institute for Basic Science Research, Chungbuk National University, Chongju 361-763, Korea; cheongho@astroph.chungbuk.ac.kr

[18]Farm Cove Observatory, Centre for Backyard Astrophysics, Pakuranga, Auckland New Zealand; farmcoveobs@xtra.co.nz

[19]Korea Astronomy and Space Science Institute, Daejon 305-348, Korea; bgpark@kasi.re.kr

[20]Universidad de Concepción, Departamento de Fisica, Casilla 160–C, Concepción, Chile

[21]Institute of Astronomy Cambridge University, Madingley Rd., CB3 0HA Cambridge, UK dmb7@ast.cam.ac.uk

[22]Princeton University Observatory, Princeton, NJ 08544, USA; bp@astro.princeton.edu

[23]Astrophysics Research Centre, School of Physics, Queen's University Belfast, Belfast BT7 1NN, UK;

ABSTRACT

We detect a Neptune mass-ratio ($q \simeq 8 \times 10^{-5}$) planetary companion to the lens star in the extremely high-magnification ($A \sim 800$) microlensing event OGLE-2005-BLG-169. If the parent is a main-sequence star, it has mass $M \sim 0.5\,M_\odot$ implying a planet mass of $\sim 13\,M_\oplus$ and projected separation of $\sim 2.7\,\mathrm{AU}$. When intensely monitored over their peak, high-magnification events similar to OGLE-2005-BLG-169 have nearly complete sensitivity to Neptune mass-ratio planets with projected separations of 0.6 to 1.6 Einstein radii, corresponding to 1.6–4.3 AU in the present case. Only two other such events were monitored well enough to detect Neptunes, and so this detection by itself suggests that Neptune mass-ratio planets are common. Moreover, another Neptune was recently discovered at a similar distance from its parent star in a low-magnification event, which are more common but are individually much less sensitive to planets. Combining the two detections yields 90% upper and lower frequency limits $f = 0.37^{+0.30}_{-0.21}$ over just 0.4 decades of planet-star separation. In particular, $f > 16\%$ at 90% confidence. The parent star hosts no Jupiter-mass companions with projected separations within a factor 5 of that of the detected planet. The lens-source relative proper motion is $\mu \sim 7$–$10\,\mathrm{mas\,yr^{-1}}$, implying that if the lens is sufficiently bright, $I \lesssim 23.8$, it will be detectable by the *Hubble Space Telescope* by 3 years after peak. This would permit a more precise estimate of the lens mass and distance, and so the mass and projected separation of the planet. Analogs of OGLE-2005-BLG-169Lb orbiting nearby stars would be difficult to detect by other methods of planet detection, including radial velocities, transits, or astrometry.

Subject headings: gravitational lensing – planetary systems – Galaxy: bulge

1. Introduction

The regions of our Solar System beyond Mars contain giant planets, as well as asteroids and comets, which are believed to be remnants of the process that formed these bodies,

c.snodgrass@qub.ac.uk

[24]Astrophysics Research Institute, Liverpool John Moores University, Twelve Quays House, Egerton Wharf, Birkenhead CH41 1LD, UK; ias,mfb,mjb@staru1.livjm.ac.uk

and also moons, which may serve as analogs to bodies involved in the late stages of planet formation. However, despite some 170 planet discoveries over the past decade, the analogous regions around other mature stars remain relatively inaccessible to us. As radial velocity (RV) survey time baselines have grown, they have begun to detect gas giants in these regions, but RV is sensitive to Neptune-mass planets only when they are much closer to their parent stars. Transit surveys are even more heavily biased toward close-in planets. Astrometric sensitivity does peak at large orbits but is fundamentally restricted to orbital periods that are shorter than the survey.

By contrast, microlensing sensitivity peaks at the Einstein ring, which is typically at 2–4 AU, depending on the mass and distance of the host star, and it extends several times farther out. Moreover microlensing detections are "instantaneous snapshots" of the system, not requiring an orbital period to elapse. Hence, microlensing can potentially yield important information about the intermediate-to-outer regions of extrasolar planetary systems that are difficult to probe by other techniques.

Gravitational microlensing occurs when a "lens" star becomes closely aligned, within an angular Einstein radius $\theta_{\rm E}$, with a more distant source star. The source is magnified by an amount that grows monotonically as it approaches the lens, and diverges inversely with separation for extremely close encounters (Einstein 1936; Paczyński 1986).

Planets hosted by the lens star induce two, generally distinct, perturbations on the single-lens magnification pattern: a small "planetary caustic" (closed contour of formally infinite magnification) directly associated with the planet and an even smaller "central caustic" closely aligned with the host. All microlensing events have the potential to probe the planetary caustic, but owing to its small extent and the random trajectory of the source, the probability for the source to encounter the perturbed region is low.

By contrast, the small fraction of events that reach very high magnification (and so small lens-source separation) *automatically* probe the region of the central caustic (Griest & Safizadeh 1998; Rhie et al. 2000; Bond et al. 2002; Rattenbury et al. 2002). Hence, even low-mass planets lying anywhere sufficiently near the Einstein ring are virtually guaranteed to perturb the light curve (Abe et al. 2004). Since the peak of the event can, at least in principle, be predicted in advance, it is possible to focus limited observing resources to make the intensive observations over the peak that are required to detect and characterize the relatively subtle signal.

The Microlensing Follow Up Network[1] (μFUN) has adopted a strategy of trying to rec-

[1]http://www.astronomy.ohio-state.edu/∼microfun/

ognize the few prospective high-magnification events among the roughly 500 microlensing events annually alerted by the Optical Gravitational Lens Experiment[2] (OGLE-III) Early Warning System (Udalski 2003) and the roughly 50 events annually alerted by the Microlensing Observations for Astrophysics[3] collaboration (MOA). During the 2005 season, this strategy led to the discovery of 2 planets. The first was the Jovian mass-ratio OGLE-2005-BLG-071Lb (Udalski et al. 2005). Here we report the second such planet, a Neptune-mass-ratio companion to the lens in OGLE-2005-BLG-169.

2. Event Discovery and Data

On 2005 Apr 21, the OGLE collaboration alerted OGLE-2005-BLG-169 as probable microlensing of a faint ($I = 19.4$) source toward the Galactic bulge, using the 1.3m Warsaw telescope in Chile (operated by the Carnegie Institution of Washington). After observations by OGLE and the 1.3m μFUN SMARTS telescope in Chile showed the event to be extremely high magnification, the observers at the 2.4m μFUN MDM telescope in Arizona interrupted their regular program to obtain more than 1000 exposures over the peak. Additional data come from the 0.35m μFUN Nustrini telescope in Auckland, New Zealand and the 2.0m PLANET/RoboNet[4] Faulkes Telescope North in Hawaii. We analyze a total of (340,22,1025,74,31) images with typical exposure times of (120,300,10,120,100) seconds in the $(I, I, I, \mathrm{clear}, R)$ passbands, respectively, from these 5 telescopes. In addition, 6 V band images from μFUN SMARTS permit determination of the source color.

All data were reduced using the OGLE data pipeline based on difference imaging analysis (DIA) (Woźniak 2000). The μFUN MDM data were also reduced using the ISIS pipeline (Alard & Lupton 1998; Alard 2000; Hartman et al. 2004). To test for any systematics in this crucial data set, we report results below derived from these two completely independent pipelines. See also Figure 1.

3. Light Curve Model

Planets are discovered in microlensing events from the brief perturbation they induce on a single-lens light curve (Mao & Paczyński 1991; Gould & Loeb 1992): $F(t) = F_{\rm s}A[u(t)]+F_{\rm b}$,

[2]http://www.astrouw.edu.pl/∼ ogle/ogle3/ews/ews.html

[3]http://www.massey.ac.nz/∼iabond/alert/alert.html

[4]http://planet.iap.fr/, http://www.astro.livjm.ac.uk/RoboNet

where $A(u) = (u^2+2)/u(u^2+4)^{1/2}$, $u(t) = (\tau^2 + u_0^2)^{1/2}$, $\tau = (t-t_0)/t_{\rm E}$, Here, $F(t)$ is the observed flux, $F_{\rm s}$ is the source flux, $F_{\rm b}$ is flux due to any unlensed background light, A is the magnification, and $\mathbf{u} = (\tau, u_0)$ is the vector position of the source normalized to $(\theta_{\rm E})$, expressed in terms of the three geometrical parameters of the event: the time of closest approach t_0, the normalized impact parameter u_0, and the Einstein timescale $t_{\rm E}$.

To describe the planetary perturbation, 3 "binary-lens" parameters are required in addition to the 3 single-lens geometric parameters $(t_0, u_0, t_{\rm E})$. These are the binary mass ratio, q, the separation of the components (in units of $\theta_{\rm E}$), b, and angle of the source trajectory relative to the binary axis, α. Finally, a seventh parameter, $\rho \equiv \theta_*/\theta_{\rm E}$, is required whenever the angular radius of the source θ_* plays a significant role, in particular, whenever the source crosses a caustic.

For planetary lenses with caustic crossings, there are 7 directly observable and pronounced light-curve features that directly constrain the 7 model parameters, up to a well-understood two-fold degeneracy (Dominik 1999) that takes $b \leftrightarrow b^{-1}$. Three of these, the epoch, duration, and height of the primary lensing event, strongly constrain $(t_0, t_{\rm E}, u_0)$. The remaining four, the two caustic-crossing times (entrance and exit) and the height and duration of one of the caustic crossings, then constrain (b, q, α, ρ).

As we now show, OGLE-2005-BLG-169 is indeed a caustic-crossing event. However, only the caustic exit (but not entrance) was well-resolved. This leads to a 1-dimensional degeneracy among the model parameters, which is then partially broken by secondary, less pronounced, features of the light curve.

The residuals to the single-lens models shown in Figure 2 exhibit a kink in slope at $\Delta t = 0.092\,$day, where Δt is the time elapsed since HJD 2453491.875 (2005 May 1 09:00). The kink is equally apparent in both sets of MDM reductions. While the *incident slope* of this kink in the light curve depends on the particular single-lens model used, the *slope discontinuity* is model-independent. Such a change in slope is induced by a caustic exit, when the trailing limb of the source crosses the caustic, causing two of its images to merge and finally vanish.

To extract model parameters, we undertake a brute-force search of parameter space. We hold the three parameters (b, α, q) fixed at a grid of values while minimizing χ^2 over the remaining four parameters, using the values of $(t_0, u_0, t_{\rm E})$ derived from the overall shape of the light curve as seeds. We find two distinct local minima that obey the $b \leftrightarrow b^{-1}$ degeneracy. These minima are embedded in elongated $\Delta\chi^2$ valleys (Fig. 3), with [α(in radians): b] axis ratio ~ 100, which occur because there are only 6 pronounced features in the light curve to constrain 7 model parameters. However, while the caustic entrance is not well resolved, the

point at $\Delta t = -0.1427\,\mathrm{day}$ does lie on this entrance and thereby singles out the solutions shown in Table 1. Nevertheless, to be conservative, we quote $3\,\sigma$ errors for light-curve parameters, which take account of both the elongated valleys and the two reductions. Most importantly,

$$q = 8^{+2}_{-3} \times 10^{-5}, \qquad b = 1.00 \pm 0.02 \qquad (3\,\sigma). \tag{1}$$

4. Mass of the Host Star and Planet

In microlensing events, the physical parameters (lens mass M, lens-source relative parallax $\pi_{\rm rel}$, and relative proper motion μ) are related to the "observable" event parameters ($t_{\rm E}$, $\theta_{\rm E}$, and the microlens parallax (Gould 2004), $\pi_{\rm E}$), by

$$\theta_{\rm E} = \sqrt{\kappa M \pi_{\rm rel}}, \quad \pi_{\rm E} = \sqrt{\frac{\kappa M}{\pi_{\rm rel}}}, \quad t_{\rm E} = \frac{\theta_{\rm E}}{\mu}, \tag{2}$$

where $\kappa \equiv 4G/(c^2\mathrm{AU})$. Of these, only $t_{\rm E}$ is routinely measurable. However, in caustic-crossing events, one can usually also measure $\theta_{\rm E}$, which both directly constrains the mass-distance relation and yields a measurement of μ. We first determine the angular source radius θ_* using the standard approach (Yoo et al. 2004a), finding $\theta_* = 0.44 \pm 0.04\,\mu\mathrm{as}$. Together with the parameter measurements $\rho = 4.4^{+0.9}_{-0.6} \times 10^{-4}$ and $t_{\rm E} = 43 \pm 4\,\mathrm{days}$, this yields $3\,\sigma$ ranges,

$$\theta_{\rm E} = \frac{\theta_*}{\rho} = 1.00 \pm 0.22\,\mathrm{mas}, \quad \mu = \frac{\theta_{\rm E}}{t_{\rm E}} = 8.4 \pm 1.7\,\mathrm{mas\,yr^{-1}}. \tag{3}$$

Another constraint comes from the upper limit on the lens flux, which cannot exceed the background flux measurement, $F_{\rm b}$ (corresponding to $I_{\rm b} = 19.8$). We also derive from the light curve a weak constraint on the microlens parallax, $\pi_{\rm E,\parallel} = -0.086 \pm 0.261$, which we include for completeness. Here, $\pi_{\rm E,\parallel} \equiv \pi_{\rm E} \cos\psi$ and ψ is the angle between the direction of lens-source relative motion and the position of the Sun at t_0 projected on the plane of the sky (Gould 2004).

These measurements, together with a Bayesian prior for the lens distances and masses from a Han & Gould (2003) Galaxy model and Gould (2000) mass function (but with a Salpeter [-2.35] slope at the high end), together with the assumption that all stellar objects along the line of sight are equally likely to harbor planets, yield a probability distribution for the lens mass. We find that the probabilities that the lens is a main-sequence star (MS), white dwarf (WD), neutron star (NS), and black hole (BH) are respectively 55%, 32%, 11%, and 2% . However, Neptune mass-ratio planets around NSs must be quite rare because the ~ 0.2 second oscillations they induce would easily show up in pulsar timing residuals. Since

BHs and NSs form by a similar process, this may also argue against BHs as the host. MSs and WDs represent different life stages of the same class of stars. If the host is a MS, then the median and 90% confidence interval for the mass and distance are given by

$$M = 0.49^{+0.23}_{-0.29}\,M_\odot, \qquad D_L = 2.7^{+1.6}_{-1.3}\,\mathrm{kpc}, \qquad (90\%\,\mathrm{confidence}) \tag{4}$$

implying that the best estimates for the planet mass and separation are $m_p = qM \sim 13\,M_\oplus$ and $r_\perp = b\theta_{\rm E} D_{\rm L} \sim 2.7\,{\rm AU}$, where $D_{\rm L}$ is the distance to the lens. Since WD masses are sharply peaked at $M \sim 0.6\,M_\odot$, the corresponding planet characteristics lie near the center of the same range. Future observations by the *Hubble Space Telescope* could distinguish between MS and WD hosts, as well as measuring the mass and distance of the former provided that the lens is brighter than $I \sim 23.8$ (Bennett & Anderson 2006).

5. Limits on other Companions

Does lens OGLE-2005-BLG-169L have planets other than OGLE-2005-BLG-169Lb? Central-caustic events allow one to address this question because all the companions to the lens star perturb the central caustic (Gaudi et al. 1998). Moreover, the combined perturbation from two planets is very nearly the sum of the separate perturbations, unless the two planets are closely aligned (Rattenbury et al. 2002; Han 2005). This allows us to subtract the perturbation from the one detected planet and apply the same search technique to the resulting (nearly single-lens) light curve to look for others. We find none, and so place upper limits on the presence of other planets. In particular, we exclude Jupiter-mass ($q = 2\times10^{-3}$) planets at projected separations within a factor 5.5 of the Einstein radius ($0.18 < b < 5.5$) and Saturn-mass planets within a factor 3.5.

6. Discussion

6.1. Low-mass Planets Are Common at Several AU

OGLE-2005-BLG-169 is one of only three high-magnification events with sensitivity to the central caustics induced by cold Neptunes. It and one other event, MOA-2003-BLG-32/OGLE-2003-BLG-219 (Abe et al. 2004), were sensitive to $q = 8 \times 10^{-5}$ planets throughout the "lensing zone" ($0.6 < b < 1.6$), while OGLE-2004-BLG-343 (Dong et al. 2006) was sensitive over 40% of the lensing zone. This implies $\langle f \rangle = 1/2.4 = 42\%$ for the expected fraction of stars hosting cold Neptunes within the lensing zone (0.4 decades of projected separation), but with very large uncertainty due to small number statistics.

However, we can improve our estimate by incorporating the detection of OGLE-2005-BLG-390Lb, which is a very similar ($b = 1.6, q = 7.6\times10^{-5}$) planet that was detected through the other (planetary-caustic) microlensing channel (Beaulieu et al. 2006). The expected number of detections of $q = 8 \times 10^{-5}$ lensing-zone planets (through this planetary-caustic channel) was $1.75f$ for 1995-1999 (Gaudi et al. 2002). We estimate that the expected number for 2000-2005 is a factor 1.5 higher based on a comparison of the survey characteristics during these two periods. Hence, the single detection through this channel yields $\langle f \rangle = 23\%$, also with large errors. If we combine the two channels, and impose a uniform prior, we find a median and 90% upper and lower limits of $f = 0.37^{+0.30}_{-0.21}$, in particular, a 90% confidence lower limit of $f > 16\%$.

6.2. Unique capabilities of microlensing

Can analogs to OGLE-2005-BLG-169Lb (with the same mass ratio and semi-major axis) be detected by other techniques, such as RV, transits, and astrometry? To make a strict comparison, it would be necessary to know three additional parameters of the event, namely the lens and source distances, $D_{\rm L}$ and $D_{\rm S}$, and the projection angle ψ of its semi-major axis a to the line of sight, i.e., $\sin\psi = r_\perp/a$ where $r_\perp$ is the projected star-planet separation. The stellar mass and semi-major axis are then related to the event parameters by $M = \theta_{\rm E}^2/\kappa\pi_{\rm rel}$ and $a = D_{\rm L}\theta_{\rm E} b \csc\psi$. Hence, assuming circular orbits, the velocity amplitude $v\sin i$ and orbital period P would be

$$v\sin i = \frac{qc\sin i}{2}\sqrt{\frac{\theta_{\rm E}\sin\psi}{b(1-x)}} \rightarrow 0.85\,{\rm m\,s^{-1}}\sqrt{\frac{\sin\psi}{(1-x)}}\sin i, \tag{5}$$

$$P = \frac{4\pi D_{\rm L}}{c}\sqrt{b^3\csc^3\psi(1-x)\theta_{\rm E}} \rightarrow 9.4\,{\rm yrs}\frac{D_{\rm L}}{2.7\,{\rm kpc}}\sqrt{\frac{1-x}{0.66}}\left(\frac{\csc\psi}{1.3}\right)^{3/2}. \tag{6}$$

Here $x \equiv D_{\rm L}/D_{\rm S}$ and the evaluations are for $\theta_{\rm E} = 1\,{\rm mas}$, $q = 8 \times 10^{-5}$ and $b = 1$. These equations imply that RV detection of OGLE-05-BLG-169Lb analogs would be extremely difficult both because of the low velocity amplitude and the long period. Similarly, the long period renders transit detection impossible unless a transit experiment of considerably longer duration than *Kepler* were organized. Finally, the amplitude of astrometric motion would be

$$\alpha = q\frac{D_{\rm L}}{D_{\rm analog}}\theta_{\rm E} b\csc\psi, \rightarrow 28\,\mu{\rm as}\,\frac{D_{\rm L}}{2.7\,{\rm kpc}}\,\frac{10\,{\rm pc}}{D_{\rm analog}}\,\frac{\csc\psi}{1.3}, \tag{7}$$

where $D_{\rm analog}$ is the distance to the local analog system. This amplitude would be easily detectable by the *Space Interferometry Mission (SIM)*, although at the typical periods, this would require an extended *SIM* mission. See Figure 4.

6.3. Neptunes or Failed-Jupiters?

Both OGLE-2005-BLG-169Lb and OGLE-2005-BLG-390Lb are in the cold outer regions of their planetary systems, with expected surface temperatures of $\sim 70\,\mathrm{K}$ and $\sim 50\,\mathrm{K}$, corresponding roughly to the environments of Saturn and Neptune, respectively. Both have Neptune/Sun mass ratios, with absolute mass estimates of $13\,M_\oplus$ and $6\,M_\oplus$, respectively. They must have a large fraction of rock and ice, but whether these are covered with a thick coat of gas, like Uranus and Neptune, or whether they are "naked" super-Earths such as are theorized to have formed the cores of Jupiter and Saturn, is unclear. If such cores formed routinely but usually failed to accrete the ambient gas before it dispersed, this would account for the high frequency of these objects (Ida & Lin 2005). Moreover, the absence of gas giants within a factor 5.5 of the OGLE-2005-BLG-169's Einstein ring is consistent with the idea that the detected planet is such a "failed Jupiter" (Laughlin et al. 2004). One could gain further clues by mapping out the mass and separation distributions of a larger sample.

We acknowledge the following support: NSF AST-042758 (AG,SD); NASA NNG04GL51G (DD,AG,RP); Polish MEiN 2P03D02124, NSF AST-0204908, NASA grant NAG5-12212 (OGLE); Polish FNP SP13/2003 (AU); NSF AST-0206189, NASA NAF5-13042 (DPB); NSF AST-007480 (A-YZ); Menzel Fellowship Harvard College Obs (BSG); SRC Korea Science & Engineering Foundation (CH); Korea Astronomy & Space Science Institute (B-GP); Marsden Fund of NZ (IAB,PCMY); Deutsche Forschungsgemeinschaft (CSB); PPARC, EU FP6 programme "ANGLES" (ŁW,SM,NJR); PPARC (RoboNet); Dill Faulkes Educational Trust (Faulkes Telescope North); Assistance by Lydia Philpott, Jan Snigula and the Computer Science Department of the University of Auckland is acknowledged. We thank the MDM staff for their support. All findings are those of the authors and do not necessarily reflect NSF views.

REFERENCES

Abe, F. et al. 2004, Science, 305, 1264

Alard, C. & Lupton, R.H., 1998, ApJ, 503, 325

Alard, C. 2000, A&A, 144, 363

Beaulieu, J.-P. et al. 2005, Nature, 439, 437

Bennett, D.P., & Anderson, J. 2006, in preparation

Bond, I. A., et al. 2002, MNRAS, 331, L19

Bond, I.A., et al. 2004, ApJ, 606, L155

Dominik, M. 1999, A&A, 349, 108

Dong, S., et al. 2006, ApJ, in press, (astroph/0507079)

Einstein, A. 1936, Science, 84, 506

Gaudi, B. S., Naber, R.M. & Sackett, P. D. 1998, ApJ, 502, L33

Gaudi, B. S., et al. 2002, ApJ, 566, 463

Gould, A. 2000, ApJ, 535, 928

Gould, A. 2004, ApJ, 606, 319

Gould, A., & Loeb, A. 1992, ApJ, 396, 104

Griest, K. & Safizadeh, N. 1998, ApJ, 500, 37

Han, C. 2005, ApJ, 629, 1102

Han, C. & Gould, A. 2003, ApJ, 592, 172

Hartman, J.D., Bakos, G., Stanek, K.Z., & Noyes, R.W. 2004, AJ, 128, 1761

Ida, S., & Lin, D.N.C. 2005, ApJ, 626, 1045

Laughlin, G., Bodenheimer, P., & Adams, F.C. 2004, ApJ, 612, L73

Mao, S. & Paczyński, B. 1991, ApJ, 374, L37

Paczyński, B. 1986, ApJ, 304, 1

Rattenbury, N. J., Bond, I. A., Skuljan, J., & Yock, P. C. M. 2002, MNRAS, 335, 159

Rhie, S. H. et al. 2000, ApJ, 533, 378

Udalski, A. 2003, Acta Astron., 53, 291

Udalski, A., et al. 2005, ApJ, 628, L109

Woźniak, P.R. 2000, Acta Astron., 50, 421

Yoo, J., et al. 2004a, ApJ, 603, 139

Table 1. Light Curve Models

Pipe-line	$\Delta\chi^2$	$t_0 - t_{\rm ref}$ day	u_0 $\times 10^3$	$t_{\rm E}$ day	b	q $\times 10^5$	α deg	ρ $\times 10^4$	$\theta_{\rm E}$ mas	μ mas/yr
DIA	0.00	0.0008	1.24	42.27	1.0198	8.6	117.0	4.4	1.00	8.6
ISIS	0.00	0.0009	1.23	42.56	1.0194	8.2	118.2	4.7	0.93	8.0
DIA	0.27	0.0004	1.25	42.09	0.9819	8.3	122.6	3.9	1.12	9.7
ISIS	2.33	0.0007	1.17	44.69	0.9825	7.3	123.5	4.0	1.11	9.0

Note. — $t_{\rm ref}$ = HJD 2453491.875 (2005 May 1 09:00).

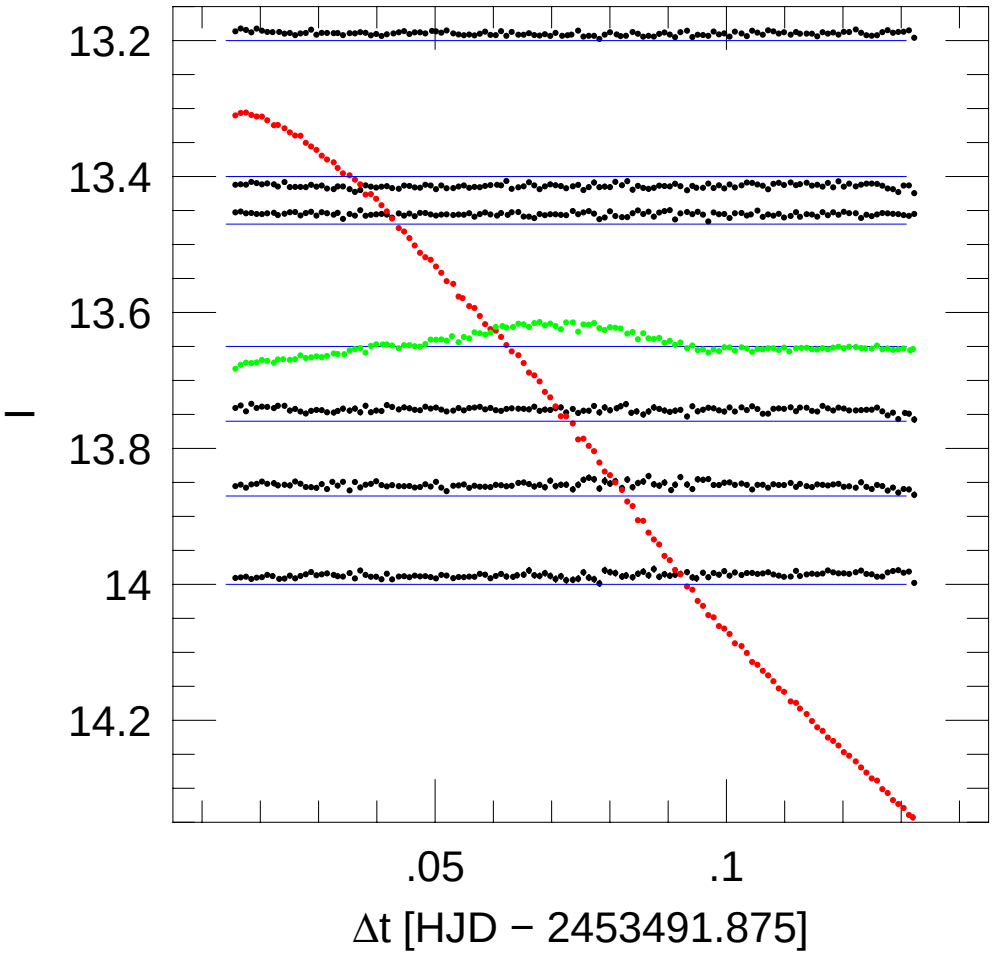

Fig. 1.— Light curves of 6 reference stars (*black*) compared to microlensed source (*red*) as derived by the DIA reductions of the MDM data. The deviation of this curve from a single-lens microlensing fit (derived from the non-MDM points) is shown in *green*. Horizontal *blue* lines are shown to aid in judging the constancy of the various stars.

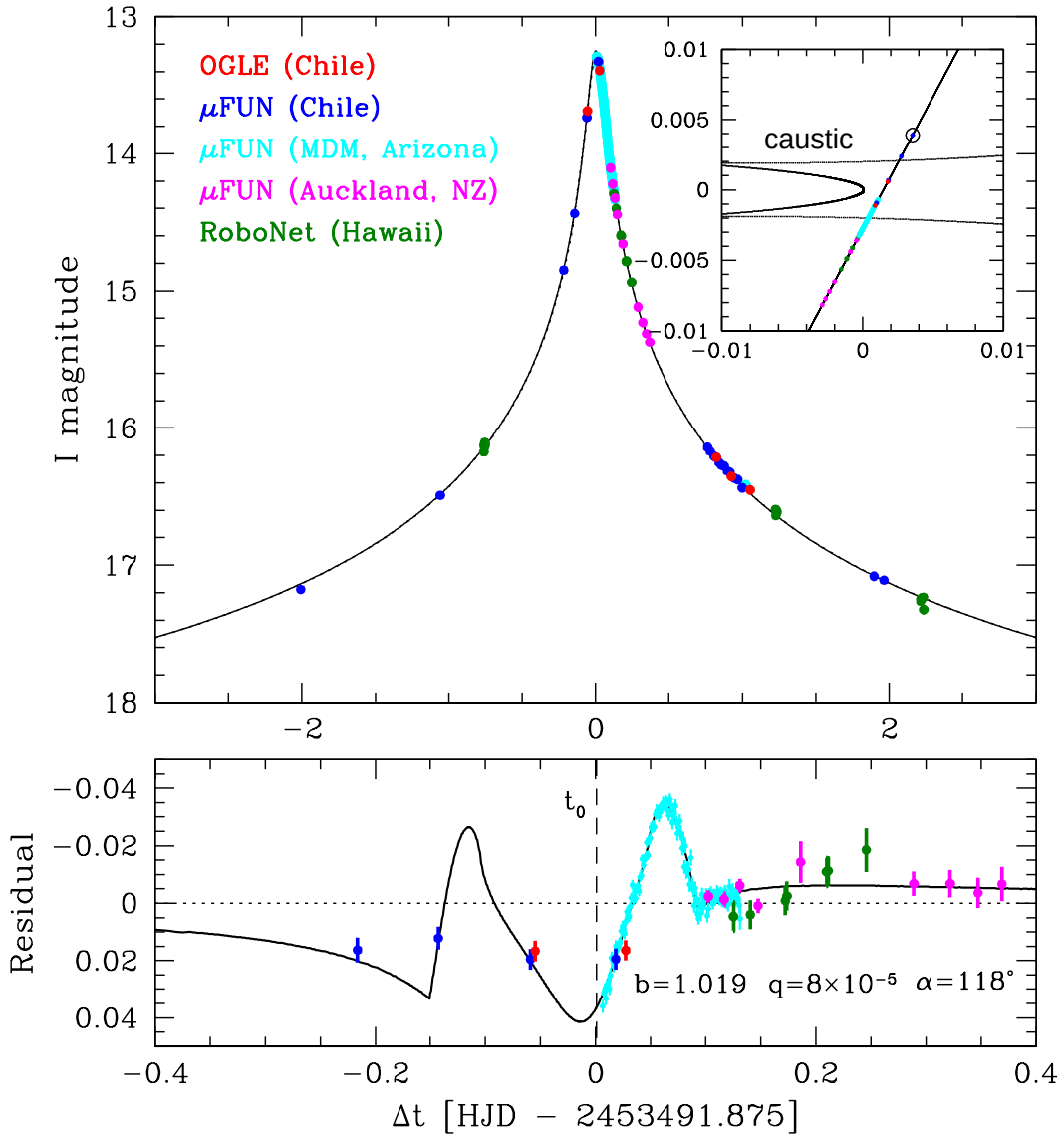

Fig. 2.— Data and best-fit model of OGLE-2005-BLG-169. Lower panel shows difference between this model and a single-lens model with the same $(t_0, u_0, t_{\rm E}, \rho)$. It displays the classical form of a caustic entrance/exit that is often seen in binary microlensing events, where the amplitudes and timescales are several orders of magnitude larger than seen here. MDM data trace the characteristic slope change at the caustic exit ($\Delta t = 0.092$) extremely well, while the entrance is tracked by a single point ($\Delta t = -0.1427$). The dashed line indicates the time t_0. Inset shows source path through the caustic geometry and indicates the source size, ρ.

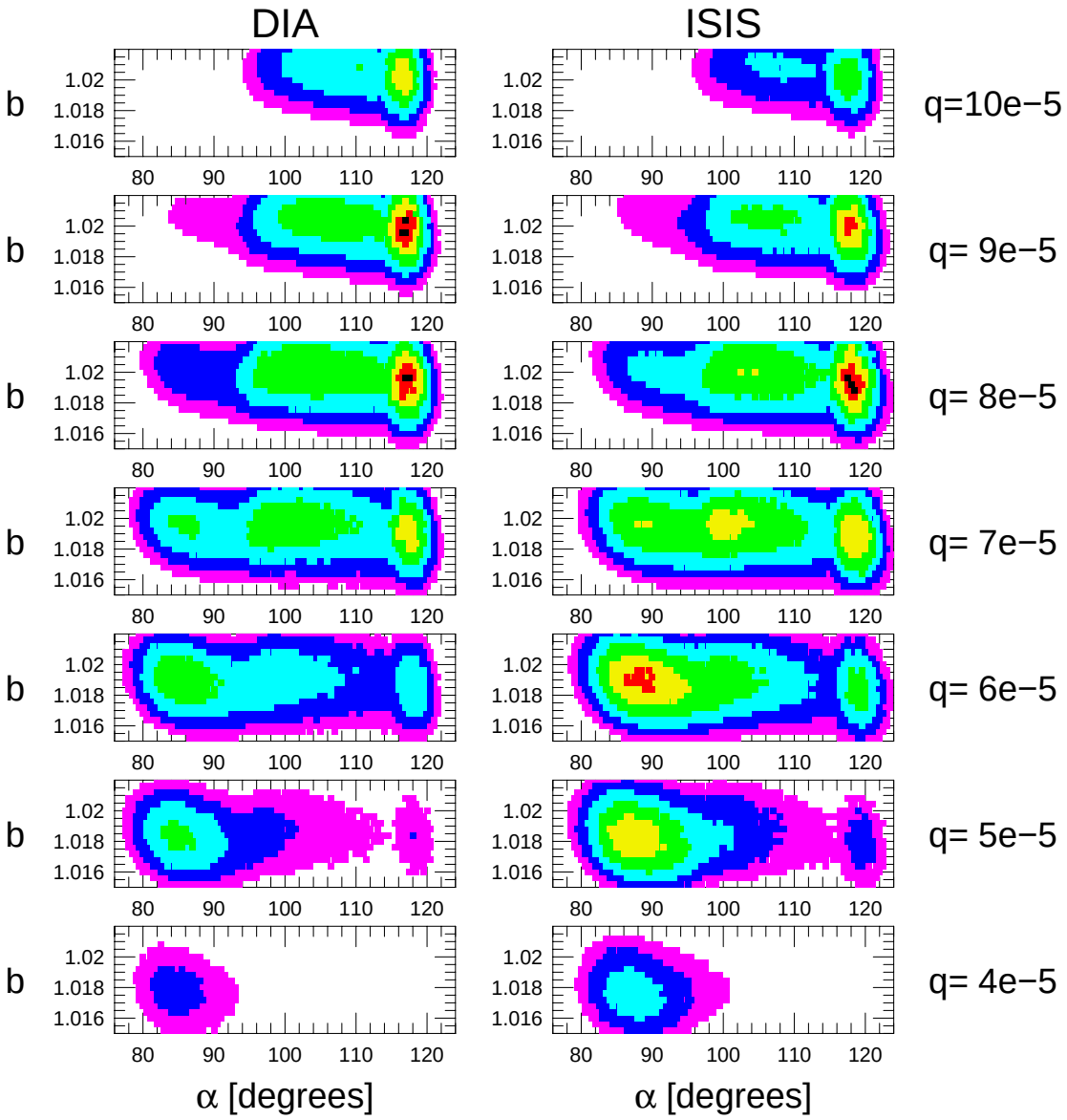

Fig. 3.— $\Delta\chi^2$ contours relative to the respective minima for light-curve fits using the DIA and ISIS reductions of the MDM data. $\sigma \equiv \sqrt{\Delta\chi^2} < 1, 2, 3, 4, 5, 6, 7$ are shown by black, red, yellow, green, cyan, blue, and magenta. Note that abscissae are compressed, so the $6\,\sigma$ contours have an axis ratio of approximately 100 (with α expressed in radians), which reflects the 1-D degeneracy discussed in the text. Both reductions have their minimum at $(\alpha, q) \sim (120°, 8 \times 10^{-5})$. Similar contours for $b < 1$ yield additional solutions that are included in Table 1. The full $3\,\sigma$ mass-ratio range is confined to 5–10$\times 10^{-5}$ even allowing for both reductions.

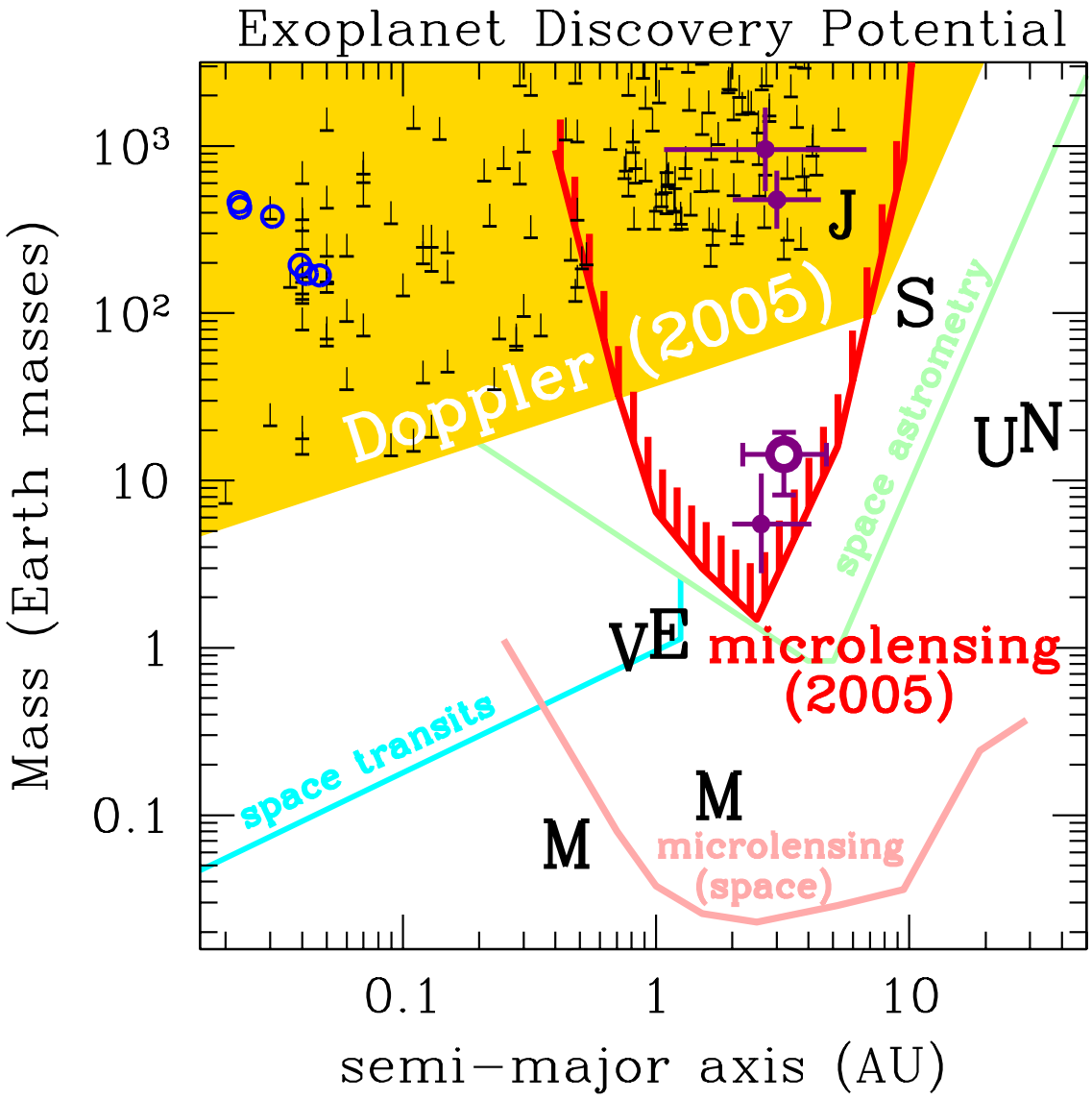

Fig. 4.— Exoplanet discovery potential and detections are shown as functions of planet mass and semimajor axis. Potential is shown for current ground-based RV (*yellow*) and, very approximately, microlensing (*red*) experiments as well as future space-based transit (*cyan*), astrometric (*green*), and microlensing (*peach*) missions. Planets *discovered* using the transit (*blue*), RV (*black*), and microlensing (*magenta*) techniques are shown as individual points, with OGLE-2005-BLG-169Lb displayed as an open symbol. Solar system planets are indicated by their initials for comparison.